Alexandria Engineering Journal (2011) 50, 219–227

Alexandria University

Alexandria Engineering Journal

www.elsevier.com/locate/aej
www.sciencedirect.com

ORIGINAL ARTICLE

Two-dimensional displacement measurement using static close range photogrammetry and a single fixed camera

Abdallah M. Khalil *

Production Engineering Department, Faculty of Engineering, Alexandria University, Alexandria 21544, Egypt

Received 20 January 2011; revised 6 July 2011; accepted 30 July 2011
Available online 28 September 2011

KEYWORDS

Two-dimensional;
Displacement;
Measurement;
Photogrammetry;
Single camera

Abstract This work describes a simple approach to measure the displacement of a moving object in two directions simultaneously. The proposed approach is based on static close range photogrammetry with a single camera and the well-known collinearity equations. The proposed approach requires neither multi-camera synchronization nor mutual camera calibration. It requires no prior knowledge of the kinematic and kinetic data of the moving object. The proposed approach was used to evaluate predefined two-dimensional displacements of a moving object. The root mean square values of the differences between the predefined and evaluated displacements in the two directions are 0.11 and 0.02 mm.

1. Introduction

Increasing demand for fast, reliable and more accurate portable coordinate measurement systems have set photogrammetry among the most suitable measurement techniques for a wide range of applications. Photogrammetry is a very versatile and reliable 3-D measurement tool, which offers a unique set of capabilities. Close range photogrammetry started achieving successful technical and economical results in the mid 1980s [1].

Photogrammetry encompasses methods of image measurement and interpretation enabling the derivation of the shape and location of an object from one or more photographs of that object [2]. One known advantage of photogrammetry is the possibility to monitor hundreds of detail points simultaneously without incurring any additional cost. Bosemann [3] classifies photogrammetric systems into four different groups: offline photogrammetry, online photogrammetry, scanning systems, and dedicated systems. In online photogrammetry, two or more high resolution digital cameras are mounted on tripods and their relative position is calculated using a calibration procedure. Points identified in the pictures are then calculated by ray intersection. Using this methodology the relative movements between the cameras and a part can be measured.

* Tel./fax: +20 3 5923743.
E-mail address: abdallah.khalil@alex.edu.eg

Peer review under responsibility of Faculty of Engineering, Alexandria University.
doi:10.1016/j.aej.2011.07.003

Production and hosting by Elsevier

Luhmann et al. [2] explain that stereo vision systems require at least two synchronized cameras for image acquisition, each with known calibration values and predetermined orientation with respect to an established coordinate system. Pollefeys et al. [4] discuss in their work some of the limitations of an accurate photogrammetric measurement system. The authors state that the calibration procedures should be minimized, image acquisition simplified and simple low-cost acquisition systems used.

In the medical field numerous researchers have used stereo vision systems for biomedical examination. Burke et al. [5] evaluated human face alterations during surgical treatment. D'Apuzzo [6] developed a method to measure and track moving surfaces of human body parts from multi-image video sequences acquired simultaneously from three synchronized CCD cameras. Another technique based on stereo-imaging was developed by Nicolella et al. [7] to measure the microstructural strain field in cortical bone. Goellner et al. [8] studied the effect of low tensile forces on tooth displacement using a two stereo-camera photogrammetric technique.

Digital photogrammetric systems have also been used to overcome the limitations of conventional measurement tools in industrial applications. Tournas et al. [9] developed a photogrammetric system comprising of two CCD cameras to monitor the deformations of concrete elements. Ergun [10] developed a similar system to evaluate the deformations in a reinforced concrete slab using stereo matching. Dold and Peipe [11] examined the suitability of digital photogrammetric systems to track and analyze object motion. The authors compare the results obtained from the V-STARS photogrammetric system to those obtained from a 3-D laser tracker.

Many researchers developed systems based on prior knowledge of the object's motion model to analyze its displacement and velocity. Kasprzak [12] describes in his work a model based approach to moving object recognition in image sequences under egomotion. The author uses a single camera to track vehicles in traffic scenes. Schindler et al. [13] developed a similar system for detecting and tracking pedestrians using a stereo camera rig mounted on a moving camera platform. The position and orientation of the stereo rig is obtained through egomotion estimation. Ambrosio et al. [14] use a single camera and a biomechanical model to reconstruct human body motion.

Luhmann et al. [2] explain the use of high speed image sequences (cinematography) to describe the kinematics of a moving object. The authors point out that cinematography is limited to applications where the object movement is closely parallel to the image plane. Chitrakaran et al. [15] state that a good amount of effort, in previous researches, is focused on developing system theory-based algorithms to estimate and compensate for unknown object kinematics. However, these methods do not seem to identify the object's velocity if not much is known about the motion of the object.

In all photogrammetric applications, the accuracy of measurement depends on the geometric reliability of the camera and the feasibility to perform accurate coordinate measurements on digital images. Camera reliability is achieved by performing a robust camera calibration procedure to estimate the interior orientation parameters. In stereo vision systems the individual camera calibrations is followed by the calibration of the combination of the two cameras [16–18].

One of the most important factors affecting the accuracy of measurements in photogrammetry is the number of camera views. In static-close-range photogrammetry one may increase the number of camera views by moving the camera and taking a number of images. In dynamic close-range photogrammetry of moving objects, the number of camera views is restricted to the number of physical cameras available [19]. Luhmann [20] emphasizes the importance of single camera solutions especially in applications confined to only one camera, e.g. due to restrictions in terms of costs, synchronization demands or spatial observation conditions.

In this paper a simple approach for the measurement of an object's movement in two directions simultaneously is proposed. The proposed approach uses a static close range photogrammetric technique with a single fixed camera and is based on the well-known collinearity equations. Before the object starts to move a number of images are taken with a single calibrated camera from several positions. The camera station corresponding to the last image taken is kept unchanged. The images taken from the different camera stations are used to evaluate the elements of exterior orientation using bundle adjustment. Once the elements of exterior orientation have been evaluated, images are taken from the fixed camera station while the object is moving. The proposed approach assumes that the object's motion is in two dimensions only. Therefore, measurement of the image coordinates corresponding to a specific point on the object can be utilized to evaluate its coordinates in object space by substitution in the collinearity equations. The proposed approach requires no pre-knowledge of the kinematic properties of the moving object since no dynamic model is used in the analysis.

2. Theoretical approach

The theoretical approach presented in this section is used to evaluate the displacement of a moving object in two directions using a single camera. The most fundamental and useful relationship in analytical photogrammetry is the collinearity condition, Fig. 1. Eqs. (1) and (2) express the collinearity condition for any point on an image: the first equation for

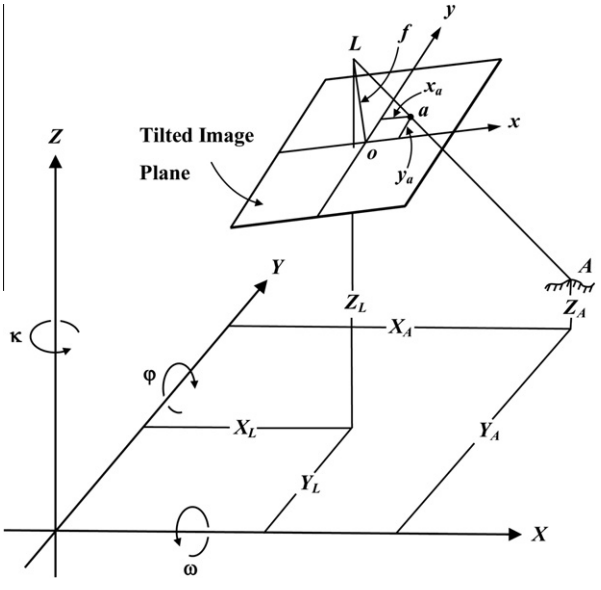

Figure 1 The collinearity condition.

the (x) image coordinate and the second for the (y) image coordinate [21].

$$x_a = x_o - f\left[\frac{m_{11}(X_A - X_L) + m_{12}(Y_A - Y_L) + m_{13}(Z_A - Z_L)}{m_{31}(X_A - X_L) + m_{32}(Y_A - Y_L) + m_{33}(Z_A - Z_L)}\right] \quad (1)$$

$$y_a = y_o - f\left[\frac{m_{21}(X_A - X_L) + m_{22}(Y_A - Y_L) + m_{23}(Z_A - Z_L)}{m_{31}(X_A - X_L) + m_{32}(Y_A - Y_L) + m_{33}(Z_A - Z_L)}\right] \quad (2)$$

In Eqs. (1) and (2), x_a and y_a are the photo coordinates of an image point a with respect to the principal point; X_A, Y_A, and Z_A are the object space coordinates of the point; X_L, Y_L, and Z_L are the object space coordinates of the camera (exposure) station; f is the camera focal length; x_o and y_o are the coordinates of the principal point; and the m's are functions of the three rotation angles. The rotation angles are defined in terms of a right-handed coordinate system by three Euler angles Omega, Phi, and Kappa.

2.1. Evaluation of object displacement

In this paper the object's two dimensional displacements are evaluated using a number of images taken from a single fixed camera. Successive images are taken of the moving object and used to evaluate the corresponding object coordinates (X_A) and (Y_A) and therefore its displacements in both the (X) and (Y) directions. To evaluate the object's coordinates (X_A) and (Y_A) and taking correction for lens distortion errors into account, Eqs. (1) and (2) are rearranged in the form given in the following equations:

$$X_A = X_L + (Z_A - Z_L)\left[\frac{m_{11}x_c + m_{21}y_c - m_{31}f}{m_{13}x_c + m_{23}y_c - m_{33}f}\right] \quad (3)$$

$$Y_A = Y_L + (Z_A - Z_L)\left[\frac{m_{12}x_c + m_{22}y_c - m_{32}f}{m_{13}x_c + m_{23}y_c - m_{33}f}\right] \quad (4)$$

where;

$$x_c = x_a - x_o + \delta x + \Delta x$$
$$y_c = y_a - y_o + \delta_y + \Delta y$$

In Eqs. (3) and (4), δx and δy are the symmetric radial lens distortion corrections and Δx and Δy are the decentering distortion corrections.

Eqs. (3) and (4) comprise a number of unknowns; the interior orientation parameters of the camera, the exterior orientation parameters of the camera station and the object space coordinates (Z_A). The interior orientation parameters which constitute of the coordinates of the principal point (x_o, y_o), the camera focal length (f), the symmetric radial distortions (δx and δy) and the decentering distortions (Δx and Δy) are all obtained from the camera calibration.

2.2. Evaluation of the exterior orientation parameters

As opposed to the more common photogrammetric motion analyses systems, the approach used in this paper is based on static photogrammetry. The elements of exterior orientation of the camera station used to capture the moving object are evaluated before the object starts to move. In order to evaluate the six elements of exterior orientation, (ω, φ and κ) and (X_L, Y_L and Z_L), a number of images are taken of the object while it is stationary. The elements of exterior orientation, for all camera stations, are evaluated using bundle adjustment [22]. The bundle adjustment procedure also yields the object space coordinates (X_A, Y_A and Z_A) of the object while it is stationary. If the object's motion is confined only to two directions in the X–Y plane then the object space coordinates (Z_A) will remain constant while the object is moving. It is most important that the camera station corresponding to the last taken image remains fixed. This last camera station will be used to capture successive images of the moving object. Once the elements of exterior orientation of the fixed camera station and the object space coordinates (Z_A) have been determined, Eqs. (3) and (4) can be used to evaluate the object's (X_A) and (Y_A) coordinates. Capturing an image of the moving object at a specific instance can therefore be used to evaluate its current location, in both the (X) and (Y) directions, by solving Eqs. (3) and (4) simultaneously.

3. Experimental work

In order to evaluate the validity of the theoretical approach presented in Section 2, the experimental procedure presented in this section is conducted. The aim of this procedure is to move an object with predefined incremental values in two directions. The known incremental displacement values are then compared to those obtained using the proposed approach.

The camera used in this work is the Canon EOS 5D digital Single-Lens Reflex (SLR) with a fixed 35 mm focal length lens. The effective number of pixels of the camera is 12.8 megapixels. The camera is calibrated using a single calibration grid.

3.1. Measurement set-up

A ToolMaker's Microscope by Carl Zeiss, shown in Fig. 2, is used to provide the known displacement values. The instrument's table can be moved in two directions, (X) and (Y), using micrometers each having a resolution of 0.01 mm. The table's movement in both the (X) and (Y) directions is evaluated using the proposed approach.

Printed circular targets are used for accurate sub-pixel marking of various points. A total of nineteen targets are used. Eleven targets are located on stationary features, either on the ToolMaker itself or other non-moving parts. Eight targets are placed on the moving table. The eight moving targets are labeled M1–M8. The moving targets have different heights to show that the proposed method is capable of tracking the displacement of various points, having different (Z) coordinates, in the (X–Y) plane simultaneously. The circular targets diameter is initially estimated using an approximate method based on the amount of coverage of the object in the images. The estimated value is found to be 2 mm. In order to increase the accuracy of sub-pixel marking, the actual target diameter used is 8 mm. Care was taken as not to use an oversized target diameter in order to reduce measurement errors [23].

Targets (M4 and M5) and (M2 and M3) are printed with two lines connecting their centers, (L1 and L2) respectively. The purpose of those lines is to match the (X) and (Y) movement directions of the ToolMaker with those defined in the collinearity equations. This is achieved in two steps, first L1

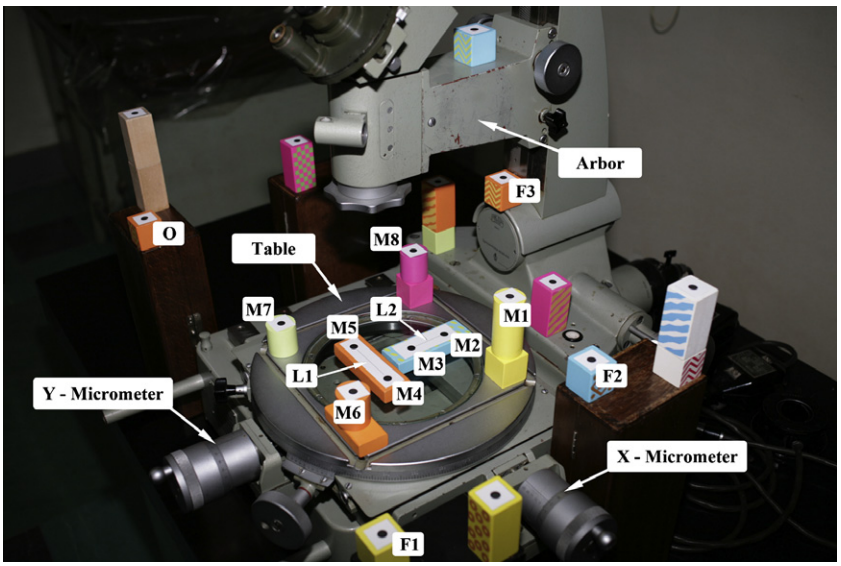

Figure 2 Measurement set-up.

and L2 are respectively aligned with the table's (X) and (Y) movement directions using the ToolMaker's goniometer ocular. Second, lines L1 and L2 shall be used to define the (X) and (Y) coordinates of the collinearity equations. To scale the values obtained from bundle adjustment into real-world dimensions, the center-distance between targets (M4 and M5) is measured on a Universal Measuring Machine by Carl Zeiss and is found to be 60.085 mm.

3.2. Evaluation of the exterior orientation parameters

Images are taken from seven different positions around the instrument, Fig. 3. The number of positions provides good coverage of the measured object and good angular separation. At each position two images are taken, one in landscape and the second in portrait. Each image has its own unique set of exterior orientation parameters and, therefore, presents a different camera station. Fourteen images, camera stations, are therefore used to evaluate the exterior orientation parameters. The image shown in Fig. 2 is the last one taken. The last camera station is kept fixed and is used to capture images of the moving table. All images taken from the fixed camera station have a fixed focusing distance and are more focused on the moving targets. Before moving the table all nineteen targets are used to evaluate the exterior orientation parameters. The software PhotoModeler Pro5 by EOS systems is used to yield the elements of exterior orientation.

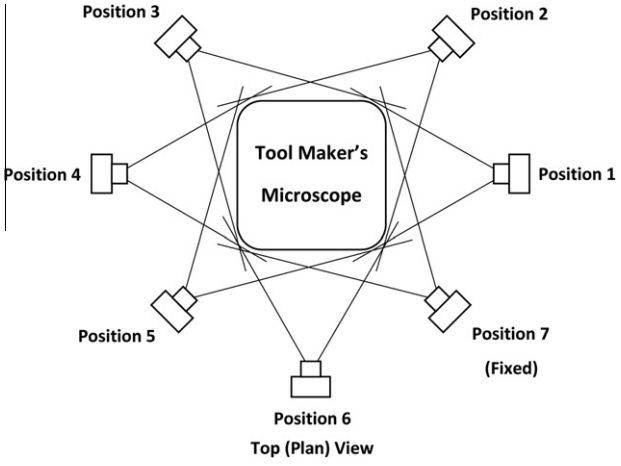

Figure 3 Camera positions.

Four groups of data, obtained from PhotoModeler, are used in the evaluation of the table movement. The first group includes the elements of exterior orientation of the fixed camera station. The second group constitutes the evaluated vertical (Z) coordinates of the marked targets (Z_A). The third group of data is the image coordinates of the marked targets. The Fourth group includes the targets marking residuals which will be used to assess the quality of targets marking. Photomodeler uses a bundle adjustment procedure to evaluate the four groups of data.

3.3. Evaluation of table movement

The (X) and (Y) micrometers are used to move the table with known displacement values. After each step movement an image is taken. The image coordinates of the moving targets obtained from PhotoModeler are used to evaluate the object space coordinates (X_A and Y_A) using Eqs. (3) and (4).

Evaluation of the table's movement may be performed based on the measurement of any of the eight moving targets. To better analyze the validity of the proposed approach, the motion of all eight moving targets is examined. Furthermore, the object space coordinates of three fixed targets (F1, F2 and F3) are evaluated. The purpose of evaluating the fixed targets coordinates is to examine the stability of the camera station between the various images.

4. Results and discussions

First an image is taken from the fixed camera station to evaluate the object space coordinates for the eleven targets (M1–M8) and (F1–F3) before the table is moved using Eqs.

(3) and (4). The instrument's table is then moved in the (X) and (Y) directions. The table's displacements are performed in 10 mm increments in the X-direction and 5 mm increments in the Y-direction. After each incremental displacement an image is taken and the corresponding object space coordinates (X_A) and (Y_A) for all eleven targets are evaluated.

4.1. Displacement results

Fig. 4 illustrates the difference between the nominal and evaluated displacement values at various nominal displacements for the moving target (M1) in both the (X) and (Y) directions. Fig. 4a shows that the differences between the nominal and evaluated X-displacement values ($X_{\text{Difference}}$) have a randomly distributed nature about the X-axis. However, the differences between the nominal and evaluated Y-displacement values ($Y_{\text{Difference}}$) have a clear linear trend; Fig. 4b.

This latter observation was expected because the X-axis is defined as the primary (dominant) axis in the software Photomodeler. When the coordinate system is computed, by the software, the (X), (Y) and (Z) axes are not exactly 90° apart. This is treated, in this paper, as a misalignment between the nominal Y-displacement direction (axis) and that computed by the software. The equation of a best-fitting line is obtained using linear regression. The slope of the best-fitting line corresponding to the displacement results of target (M1) is found to be 0.030. The same procedure is repeated for moving targets (M2–M8), Table 1 lists their corresponding best-fitting line slopes. The slope values listed in Table 1 have almost identical values with the exception of that corresponding to target (M8). The equation of the best fitting line, for each of the moving targets, is used to compensate for the misalignment error in the difference between the nominal and evaluated Y-displacement values ($Y_{\text{Difference}}$).

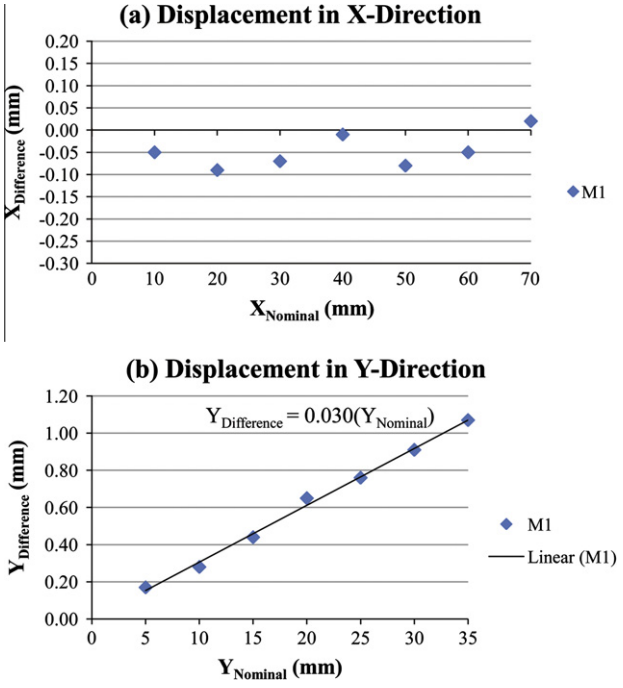

Figure 4 Difference between nominal and evaluated displacement values for target M1.

Fig. 5 illustrates the relationship between ($X_{\text{Difference}}$) and (X_{Nominal}) for all moving targets. For clarity purposes Fig. 5a illustrates the relationships for targets (M1–M4) while Fig. 5b illustrates those for targets (M5–M8). The results obtained for all eight targets show almost identical trends with the exception of target (M8). Fig. 6 illustrates the relationship between ($Y_{\text{Difference}}$), after the correction for the misalignment error, and (Y_{Nominal}). Fig. 6a illustrates the relationships for targets (M1–M4) while Fig. 6b illustrates those for targets (M5–M8). The results obtained for all eight targets show almost identical trends. Once again with the exception of target (M8). Examining the location of target (M8) in Fig. 2 shows that moving the table in the X-direction brings target (M8) below the arbor of the ToolMaker's Microscope. The shadow of the arbor falling on target (M8) reduced the accuracy of target marking to a large extent. This explains why the results of only the first three X-displacements (Fig. 5b) and first four Y-displacements (Fig. 6b) are in good agreement with those of the other moving targets. The displacement results reported for target M8 show the need for a more homogeneous and consistent illumination method during the course of measurement.

4.2. Effect of target marking precision

In order to examine the effect of target marking precision on the obtained results, the root mean square (RMS) marking residuals are examined. Table 2 lists the RMS residual values, obtained from PhotoModeler, for all targets. Although target (M8) has a relatively small RMS residual, it is excluded due to the previously mentioned reason. The four moving targets having the smallest RMS residual values, excluding target (M8), are (M2, M3, M4 and M5). Figs. 7 and 8 illustrate the displacement results for the four targets in both the (X) and (Y) directions, respectively. Initial examination of Figs. 7 and 8 shows that the results corresponding to those four targets have very similar trends. Further examination reveals that the two targets having the smallest RMS residuals (M2 and M4) have almost identical values in Fig. 7 and exactly equal values in Fig. 8. It can therefore be concluded that the target RMS marking residual has a direct impact on the accuracy of the evaluated displacement values. Therefore, target (M2) is used to describe the most accurate results.

4.3. Comparison between displacement results in both directions

Table 3 lists the maximum and the RMS values of the difference between the nominal and evaluated displacements, in the (X) and (Y) directions, for target (M2). The maximum

Table 1 Best-fitting lines slope values.

Target	M1	M2	M3	M4	M5	M6	M7	M8
Slope	0.030	0.029	0.029	0.028	0.028	0.028	0.028	0.025

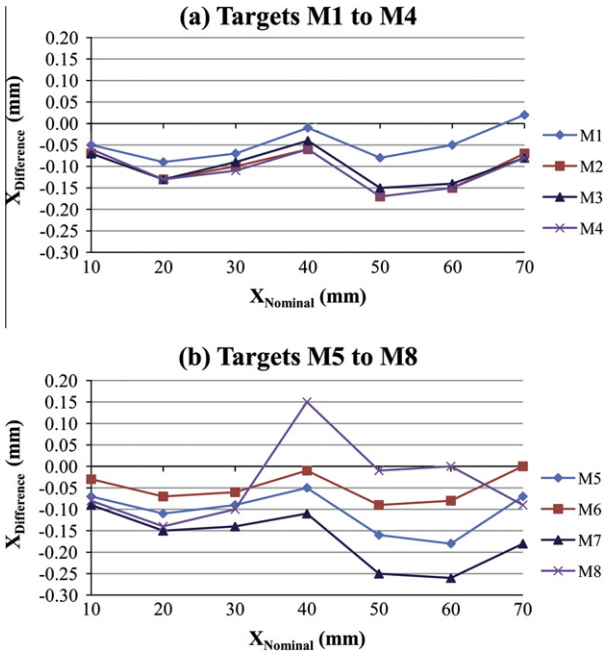

Figure 5 Relationship between X_{Nominal} and $X_{\text{Difference}}$.

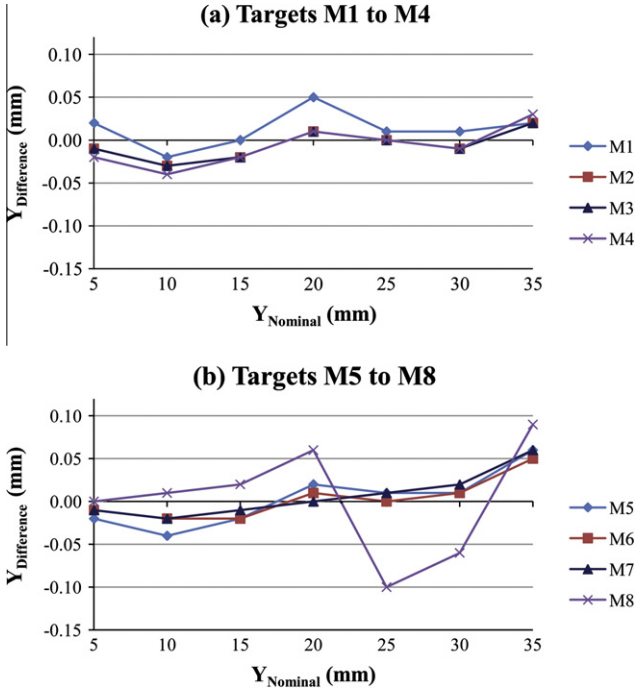

Figure 6 Relationship between Y_{Nominal} and $Y_{\text{Difference}}$.

differences being recorded at nominal (X) and (Y) displacement values of 50 mm and 10 mm, respectively.

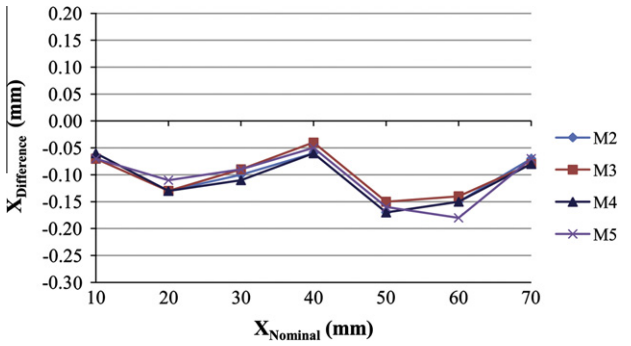

Figure 7 Relationship between X_{Nominal} and $X_{\text{Difference}}$ (Targets M2–M5).

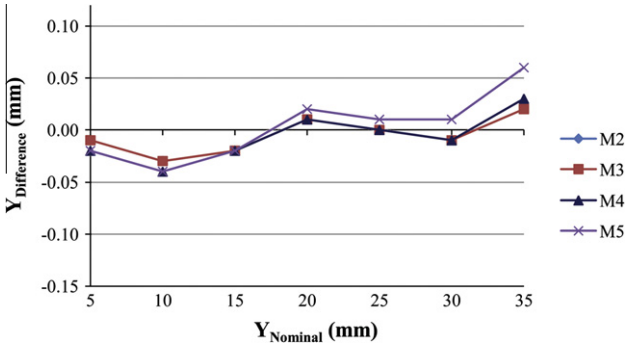

Figure 8 Relationship between Y_{Nominal} and $Y_{\text{Difference}}$ (Targets M2–M5).

Table 3 Maximum and RMS differences for target M2.

Displacement direction	Maximum difference (mm)	RMS (mm)
X	−0.17	0.11
Y	−0.03	0.02

Clearly the maximum difference recorded in the X-direction is relatively larger than that recorded in the Y-direction. The same observation applies to all moving targets. This clearly points out that the accuracy of evaluation of (Y_A) is higher than that of (X_A). Eqs. (3) and (4) show that, for a specific image coordinate (x_c, y_c), all variables used to evaluate (X_A) and (Y_A) are equal except for the (m) values in the numerator of both equations and the coordinates (X_L and Y_L). The camera station coordinates, (X_L) and (Y_L), are both obtained during bundle adjustment and are not changed during the evaluation of the coordinates of the various points. Therefore, errors in (X_L) and (Y_L) should have a constant effect on all evaluated points. The second factor affecting the accuracy of evaluation of (X_A) and (Y_A) is the effect of the rotation angles (ω, φ and κ). Examination of the direction of the Y-displacement in Fig. 2 reveals that it is more parallel to the horizontal direction

Table 2 Targets RMS marking residuals.

Target	M1	M2	M3	M4	M5	M6	M7	M8	F1	F2	F3
RMS residual (pixels)	0.9596	0.3483	0.4314	0.4002	0.4860	0.7530	0.8650	0.4119	1.6070	1.2669	0.9290

of the image while that of the X-displacement is more parallel to its vertical direction. This can be also indicated by the value of angle (κ) which was obtained from bundle adjustment and was found to be 37.355°. This was noticed while selecting the position for the last camera station; nevertheless, this orientation was used so that all targets can be viewed in the image frame.

To further investigate the accuracy of evaluation of (X_A) and (Y_A), the relationship between the object space coordinates and their corresponding image coordinates is examined. Eleven theoretically suggested points are used in the examination. One point is at the origin of the object space coordinate system (O), five points have variable (X_A) coordinates and five points have variable (Y_A) coordinates. The incremental change in both the (X_A) and (Y_A) coordinates is 10 mm and the (Z_A) coordinate for all suggested points is zero. The image coordinates (x_a, y_a) and the distance from the principal point (r) for all eleven points are evaluated.

Fig. 9 illustrates the relationship between each of the object space coordinate (X_A and Y_A) and the corresponding distance from the image point to the principal point (r) in both the (X) and (Y) directions. The figure shows that the variation in (r) corresponding to a specific (Y_A) variation is larger than that corresponding to the same (X_A) variation. This indicates that, for a specific image coordinate measurement accuracy, the accuracy of evaluation of (Y_A) is higher than that of (X_A). It is expected that if angle (κ) was closer to 45° then the accuracy of evaluation of (X_A) and (Y_A) will be more similar.

The displacement results for target (M2) in the (X) and (Y) directions, shown in Fig. 7 and 8, are compared to each other in Fig. 10. Fig. 10 illustrates the values of ($X_{\text{Difference}}$), ($Y_{\text{Difference}}$) and the difference between them ($X_{\text{Difference}} - Y_{\text{Difference}}$) for the seven nominal displacements in the X-direction and the seven nominal displacements in the Y-direction. Fig. 10 shows that although the values for ($X_{\text{Difference}}$) and ($Y_{\text{Difference}}$) follow very similar trends, the difference between them ($X_{\text{Difference}} - Y_{\text{Difference}}$) is not constant. It can also be seen that values for ($X_{\text{Difference}} - Y_{\text{Difference}}$) do not show a continuously increasing trend as may be suggested by the values illustrated in Fig. 9. It can therefore be concluded that both the camera station coordinates (X_L, Y_L) and rotation angles (ω, φ and κ) have simultaneous effect on the accuracy of results obtained in the (X) and (Y) directions.

4.4. Effect of camera shake

If the camera was totally fixed during all image captures, then the evaluated fixed targets (F1, F2 and F3) displacements should be zero. Evaluated displacement values for the fixed targets therefore indicate an error in the in the X-direction (X_{Error}) and Y-direction (Y_{Error}). Table 2 shows that target (F1) has a relatively high RMS marking residual and therefore only targets (F2 and F3) are examined. Fig. 11 illustrates the (X_{Error}) values recorded at the various nominal displacement values (X_{Nominal}). The (X_{Error}) values show an identical trend to that of the moving targets ($X_{\text{Difference}}$) shown in Fig. 7. Similarly the (Y_{Error}) values, shown in Fig. 12, have an identical trend to that of the moving targets ($Y_{\text{Difference}}$), shown in Fig. 8, with the exception of the last point corresponding to a nominal Y-displacement of 35 mm.

It can therefore be concluded that the differences between the evaluated and nominal (X) and (Y) displacement values, ($X_{\text{Difference}}$) and ($Y_{\text{Difference}}$) respectively, are to a large extent caused by camera shake between the various image captures.

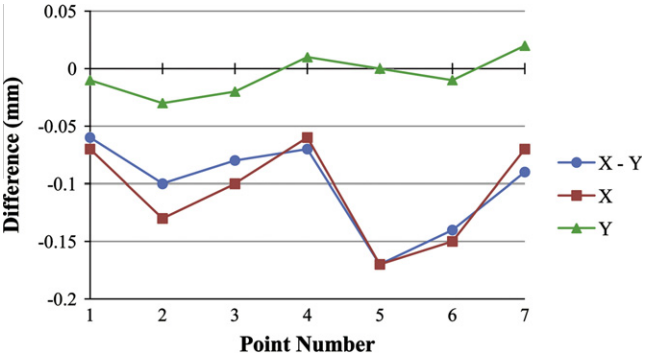

Figure 10 Comparison between $X_{\text{Difference}}$ and $Y_{\text{Difference}}$.

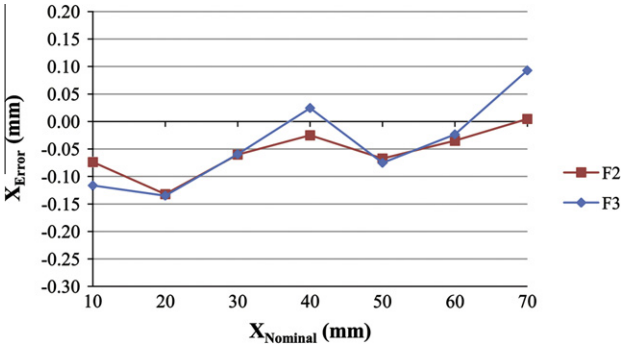

Figure 11 Relationship between X_{Nominal} and X_{Error}.

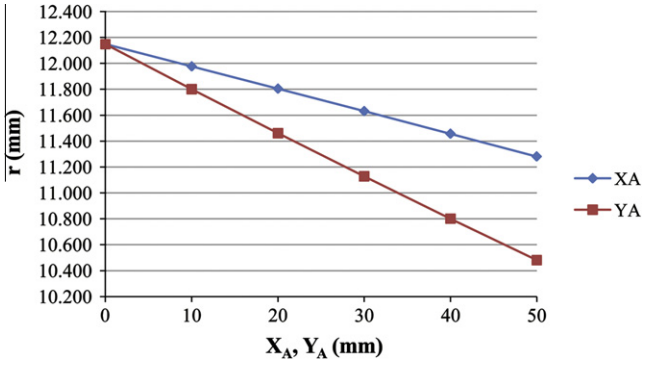

Figure 9 Relationship between (X_A, Y_A) and r.

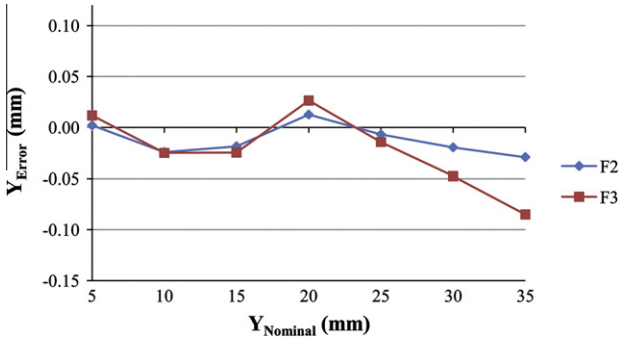

Figure 12 Relationship between Y_{Nominal} and Y_{Error}.

The (X_{Error}) and (Y_{Error}) values may therefore, be used to further enhance the accuracy of the obtained results by using them to correct their corresponding evaluated displacement values. This latter suggestion was not implemented because the RMS marking residuals of the fixed targets are relatively higher than those of the moving targets. In the present work, the camera was fixed using a commercial tripod. It is expected that more accurate results will be obtained by using a more robust fixation method. Furthermore, some deviation between the nominal and evaluated displacement values may be attributed to errors in the ToolMaker's microscope itself. The ToolMaker's micrometers were not calibrated to evaluate their inherent errors.

The results obtained show that the level of accuracy obtained is sufficient for a wide range of industrial applications. A much higher degree of accuracy can be achieved by adopting well known photogrammetry techniques. These include the use of a higher resolution camera, use of retro-reflective coded targets and taking more images of the object while it is stationary. Increasing the number of images taken while the object is stationary will increase the accuracy of the evaluated exterior orientation parameters. The accuracy of the evaluated interior orientation parameters of the camera may also be increased by performing a field calibration.

5. Conclusions

In this work a simple approach for measuring the displacement of a moving object in two directions simultaneously is presented. The proposed approach is based on static close range photogrammetry with a single camera and on the well-known collinearity equations. Predefined incremental displacements of a moving object in two perpendicular directions have been evaluated. The RMS values of the difference between the predefined and evaluated displacements, in the two directions, are 0.11 and 0.02 mm. Displacement of several objects in two perpendicular directions can be tracked simultaneously. Neither the heights of the tracked objects have to be equal nor their direction of motion be parallel to the image plane. Level of accuracy achieved is sufficient for a wide range of industrial applications. Better accuracy can be achieved by using higher resolution cameras, retro-reflective coded targets and taking more images of the object. Neither multi-camera synchronization nor mutual camera calibration was required. The number of camera views, in the proposed approach, is practically unlimited.

The proposed approach is simpler to implement and has a higher accuracy potential than single camera displacement measurement systems based on a dynamic model that require accurate kinematic and kinetic data of the moving object. The proposed approach can be used to perform on-line measurements which are currently limited to stereo vision systems. It is also well suited for applications requiring displacement monitoring over long periods of time.

The effect of rotation angles, special depth, image scale, and image convergence on the accuracy of results obtained is currently under further investigation.

Acknowledgements

The author wishes to thank Dr. Bon A. Dewitt, Associate Professor of Geomatics at The University of Florida, for his valuable suggestions concerning the mathematical foundation upon which this work was built.

He also wishes to thank his three-year old son Mostafa for letting him borrow his cube toys which were part of the measurement set-up.

References

[1] T. Luhmann, Close range photogrammetry for industrial applications, ISPRS Journal of Photogrammetry and remote sensing, in press, doi:10.1016/j.isprsjprs.2010.06.003.
[2] T. Luhmann, S. Robson, S. Kyle, I. Harley, Close Range Photogrammetry Principles, Methods, and Applications, first ed., Whittles publishing, Dunbeath, Scotland, 2007.
[3] W. Bosemann, Advances in photogrammetric measurement solutions, Computers in Industry 56 (8) (2005) 886–893.
[4] M. Pollefeys, R. Koch, M. Vergauwen, L. Van Gool, Automated reconstruction of 3D scenes from sequences of images, ISPRS Journal of Photogrammetry & Remote Sensing 55 (4) (2000) 251–267.
[5] P. Burke, P. Banks, L. Beard, J. Tee, C. Hughes, Stereophotographic measurement of change in facial soft tissue morphology following surgery, British Journal of Oral Surgery 21 (4) (1983) 237–245.
[6] N. D'Apuzzo, Surface measurement and tracking of human body parts from multi-image video sequences, ISPRS Journal of Photogrammetry & Remote Sensing 56 (5–6) (2002) 360–375.
[7] D.P. Nicolella, A.E. Nicholls, J. Lankford, D.T. Davy, Machine vision photogrammetry: a technique for measurement of microstructural strain in cortical bone, Journal of Biomechanics 34 (1) (2001) 135–139.
[8] M. Goellner, J. Schmitt, M. Karl, M. Wichmann, S. Holst, Photogrammetric measurement of initial tooth displacement under tensile force, Medical Engineering & Physics 32 (8) (2010) 883–888.
[9] L. Tournas, M. Tsakiri, M. Kattis, Displacement monitoring at the micron level using digital photogrammetry, in: 3rd IAG/12th FIG Symposium, Baden, May 22–24, 2006.
[10] B. Ergun, An expert measurement system for photogrammetric industrial applications, Measurement 39 (5) (2006) 415–419.
[11] J. Dold, J. Peipe, High resolution data acquisition to observe moving objects, International Archives of Photogrammetry and Remote Sensing 31 (B5) (1996) 471–474.
[12] W. Kasprzak, Ground plane object tracking under egomotion, International Archives of Photogrammetry and Remote Sensing 30 (5W1) (1995) 208–213.
[13] K. Schindler, A. Ess, B. Leibe, L. Van Gool, Automatic detection and tracking of pedestrians from a moving stereo rig, ISPRS Journal of photogrammetry and remote sensing, in press, doi:10.1016/j.isprsjprs.2010.06.006.
[14] J. Ambrosio, J. Abrantes, G. Lopes, Spatial reconstruction of human motion by means of a single camera and a biomechanical model, Human Movement Science 20 (6) (2001) 829–851.
[15] V.K. Chitrakaran, D.M. Dawson, W.E. Dixon, J. Chen, Identification of a moving object's velocity with a fixed camera, Automatica 41 (3) (2005) 553–562.
[16] L. Song, X. Qu, Y. Yang, Y. Cheng, S. Ye, Application of structured lighting sensor for online measurement, Optics and Lasers in Engineering 43 (10) (2005) 1118–1126.
[17] Y. Weng, P. Cohen, M. Herniou, Camera calibration with distortion models and accuracy evaluation, IEEE Transactions on Pattern Analysis and Machine Intelligence 14 (10) (1992) 965–980.
[18] L.M. Song, M.P. Wang, L. Lu, H.J. Huan, High precision camera calibration in vision measurement, Optics & Laser Technology 39 (7) (2007) 1413–1420.
[19] I.D. Wallace, N.J. Lawson, A.R. Harvey, J.D. Jones, A.J. Moore, High-speed close-range photogrammetry for dynamic

shape measurement, in: 26th International Congress on High-speed Photography and Photonics, vol. 5580, 2005, pp. 358–366.
[20] T. Luhmann, Precision potential of photogrammetric 6DOF pose estimation with a single camera, ISPRS Journal of Photogrammetry and Remote Sensing 64 (3) (2009) 275–284.
[21] P.R. Wolf, B.A. Dewitt, Elements of Photogrammetry with Applications in GIS, third ed., McGraw-Hill, Boston, USA, 2000.
[22] S.I. Granshaw, Bundle adjustment methods in engineering photogrammetry, The Photogrammetric Record 10 (56) (1980) 181–207.
[23] J. Dold, Influence of large targets on the results of photogrammetric bundle adjustment, International Archives of Photogrammetry and Remote Sensing 31 (B5) (1996) 119–123.